PHASE EQUILIBRIA STUDIES IN THE SLAG SYSTEM TiO_2-CaO-MgO–Al_2O_3-SiO_2 AT CARBON SATURATION

Baojun Zhao, Evgueni Jak & Peter Hayes
The University of Queensland, Australia

ABSTRACT

In the present laboratory-based study research methodologies have been developed that enable phase equilibria and liquidus temperatures to be measured in complex slag systems. These techniques have been employed to produce a series of phase diagrams describing liquidus temperatures at selected sections in the system "TiO_2"-(CaO-MgO)-(Al_2O_3-SiO_2) at fixed (CaO/MgO) and (Al_2O_3/SiO_2) ratios at carbon saturation.

With addition of "TiO_2" to normal iron blast furnace CaO-MgO-SiO_2-Al_2O_3 slag the liquidus temperatures and primary phase fields in the quinary system are markedly different from the system CaO-MgO-SiO_2-Al_2O_3. Two new phases perovskite $CaO\cdot TiO_2$ and pseudobrookite [$2(Ti^{3+},Mg^{2+},Al^{3+})\cdot Ti^{4+}O_5$)] are formed in the quinary system. The liquidus temperature is shown to be dependent on the (CaO+MgO)/(SiO_2+Al_2O_3), MgO/CaO and Al_2O_3/SiO_2 ratios and "TiO_2" concentration. Limited addition of "TiO_2" decreases liquidus temperatures of the slag and stability of the Ca_2SiO_4 phase. The liquidus temperatures of the iron blast furnace titaniferrous slags can be significantly decreased with increasing MgO/CaO ratio.

INTRODUCTION

The search for optimum slag composition with low melting temperatures for the blast furnace has long been the target for iron makers. Whilst historically compositions are influenced by the characteristics of commercially available ores, fluxes and fuels, in general, the targets are to minimise slag mass and operating temperature whilst satisfying requirements for sulphur and alkali removal, and slag tapping [1, 2]. The principal components of current iron blast furnace slags are described by the system Al_2O_3-CaO-MgO-SiO_2 [3, 4].

In recent years considerable thought has been devoted to lowering the environmental impact of ironmaking, in particular, reducing the energy requirements and greenhouse gas emissions from these processes. Significant reductions in CO_2 emissions can be achieved through lowering the operating temperature of the blast furnace. A key factor in achieving the low energy target is lowering the tapping temperature of the slags. Addition of small amount of TiO_2 to slags is used industrially at high temperature operating conditions to extend the life of furnace linings [5, 11]. It was reported by Fine and Arac [12] that TiO_2 addition increases the liquidus temperature of CaO-SiO_2-MgO-Al_2O_3 slags, while most of other researchers reported that liquidus temperatures are actually decreased [11, 13,14].

Phase equilibrium data are available for the system Al_2O_3-CaO-MgO-SiO_2 [3]. Muan and Osborne [4] examined the effect of substitution of 5 wt% TiO_2 for Al_2O_3 by comparing the liquidus isotherms in these respective sections. The analysis indicated that, at these high oxygen partial pressures, the replacement of Al_2O_3 by TiO_2 does not greatly change the slag liquidus temperatures.

Research on phase equilibria in the various combinations of binary and ternary subsystems of the Al-Ca-Mg-Si-Ti-O system prior to 1993 is summarised in the Slag Atlas [4]. More recent work is reported in [15, 16, 17, 18, 19], however, none of these studies provide the information on the liquidus surfaces in the composition and oxygen partial pressure ranges relevant to the industrial iron blast furnace slags.

A number of researchers [20, 21, 22, 23, 24, 25, 26] have examined the activities of TiO_2 in fully liquid metallurgical slag systems. Although scientifically useful, these data can not provide accurate information on phase liquidus surfaces of slags that may be used in industrial ironmaking practice.

Slag viscosity measurements have indicated that Ti_2O_3 concentrations up to approximately 10 wt% in a typical blast furnace slag reduce the liquidus temperatures and the viscosities of slags under reducing conditions [11, 27, 28], although the flow phenomena become more complex with the formation of TiC solids [29].

There have been no direct measurements of the phase equilibria and liquidus of the system Al_2O_3-CaO-MgO-SiO_2-TiO_2-Ti_2O_3 at low oxygen partial pressures, in the range of compositions relevant to blast furnace ironmaking. This is the type of information required in order to select the optimum compositions for the proposed low temperature, low energy blast furnace operations. This lack of information is a result of experimental difficulties encountered by earlier researchers, a situation that can be overcome by the use of the recent advances in techniques and microanalytical facilities.

METHODOLOGY

The experimental method used in the present study involves high temperature equilibration, quenching and electron probe X-ray microanalysis (EPMA). The experimental procedure is similar to those described in previous publications by the authors [30, 31].

Phase diagrams of the multi–component systems have to be presented in a form of pseudo-ternary section. Appropriate selection of the form of pseudo-ternary sections is important for efficient research and industrial application of this experimental information. In the present study of the system TiO_2-CaO-MgO-SiO_2-Al_2O_3 pseudo-ternary sections TiO_2–(CaO+MgO)–(SiO_2+Al_2O_3) have been constructed. The apexes of the pseudo-ternary section are TiO_2, (CaO+MgO) and (SiO_2+Al_2O_3). The weight ratios of MgO/CaO and Al_2O_3/SiO_2 are fixed at each section so that (CaO+MgO) or (SiO_2+Al_2O_3) can be considered as one component. These ratios are close to those in the iron blast furnace slags with [32] and without titania [1, 2, 3, 4]. In this way the systematic variation of liquidus with the basicity of the slag, i.e., (CaO+MgO)/(SiO_2+Al_2O_3) ratio can be readily examined.

A series of synthetic slags were prepared from high purity (99+%) MgO, SiO_2, Al_2O_3, $CaCO_3$ and TiO_2 powders. The mixtures were pelletised and approximately 0.2 g pellet was placed in a graphite crucible (10mm diameter and 10mm high). The crucible was placed in a basket made from pure Mo wire. Equilibration experiments were carried out in an atmosphere of ultra high purity Ar gas in a vertical recrystallised alumina reaction tube heated by lanthanum chromite elements (PYROX, France). The crucible containing the sample was suspended by Mo wire. The samples were equilibrated at predetermined temperatures for times from 1 to 16 hours depending on the slag composition and temperature, and then quenched into ice-cooled water. Reaction time has been tested at the beginning of the project to ensure that phase equilibrium has been achieved.

The quenched samples were mounted with epoxy resin and polished for metallographic examination. The polished samples were coated with carbon using a JEOL (Japan Electron Optics Ltd) Carbon Coater for electron microscopic examination. A JXA 8200 Electron Probe Microanalyser with Wavelength Dispersive Detectors was used for further analysis. The analysis was conducted at an accelerating voltage of 15 kV and a probe current of 15 nA. The ZAF correction procedure supplied with the electron probe was applied. The standards used for EPMA include alumina (Al_2O_3) for Al, magnesia (MgO) for Mg, rutile (TiO_2) for Ti and wollastonite ($CaSiO_3$) for Ca and Si. These standards were provided by Charles M Taylor Co., Stanford, California, USA. The average accuracy of the EPMA measurements is within ±1 wt %. Under experimental conditions used in the present study there may be Ti^{4+}, Ti^{3+} and Ti^{2+} present in the samples. However, only the metal cation ratios can be measured using the EPMA; the phase compositions were recalculated to TiO_2 in this paper for presentation purpose.

An important feature to note for the systems under investigation is that the compositions of the solid primary phases do not have the same Al_2O_3/SiO_2 and MgO/CaO ratios as the liquid phase present in the pseudo-ternary section. The precipitation of these crystals from the melt results in the selective removal of the components from the slag phase. This means that on crystallisation the compositions of the remaining liquids move out of the selected section. The greater the proportion of the solid phase formed, the further the liquid composition is moved away from the section. The approach that has been adopted in the present study is to select possible conditions where a low fraction of solid phase occurs. Although experiments were carefully planned, the liquid compositions at or near to the selected ratios, in general, cannot be achieved with the first experiment. This means that experiments in these primary phase fields must be repeated several times before the results on the desired pseudo-ternary sections are obtained.

RESULTS AND DISCUSSION

Descriptions of the Pseudo-ternary Sections

The compositions of the liquid and solid phases present in the quenched samples were measured using EPMA. These data have been used to construct liquidus isotherms of the pseudo-ternary sections TiO_2-(CaO+MgO)-(SiO_2+Al_2O_3) with fixed MgO/CaO and Al_2O_3/SiO_2 weight ratios. 4 pseudo-ternary sections have been investigated in this study with MgO/CaO weight ratios of 0.20, 0.20, 0.40 and 0.72 and corresponding Al_2O_3/SiO_2 weight ratios of 0.40, 0.60, 0.40 and 0.40 respectively. Figures 1 to 4 show the experimentally determined isotherms of the pseudo-ternary sections at 50 K intervals.

In these figures the experimentally determined phase boundaries are marked with thick full lines. The boundaries marked with dashed lines indicate the estimated positions of these boundaries. The thin full lines are experimentally determined isotherms and dashed thin lines indicate the estimated isotherms.

The pseudo-ternary sections are characterised by the presence of the following primary phase fields in the composition range investigated:

Section 1. TiO_2-(CaO+MgO)-(SiO_2+Al_2O_3) with Al_2O_3/SiO_2 = 0.40 and MgO/CaO = 0.20

Dicalcium silicate $2(Ca,Mg)O{\cdot}SiO_2$; merwinite $3CaO{\cdot}MgO{\cdot}2SiO_2$; melilite $2CaO{\cdot}(MgO,Al_2O_3){\cdot}2(SiO_2,Al_2O_3)$; anorthite $CaO{\cdot}Al_2O_3{\cdot}2SiO_2$, perovskite $CaO{\cdot}TiO_2$, pseudobrookite M_3O_5 and mullite $3(Al,Ti)_2O_3{\cdot}2SiO_2$. EPMA analyses show that the pseudobrookite M_3O_5 can be expressed as $2(Ti^{3+}, Mg^{2+}, Al^{3+}){\cdot}Ti^{4+}O_5$. Concentrations of Ti^{3+}, Mg^{2+} and Al^{3+} in M_3O_5 depend on the bulk composition of the slag and temperature.

Section 2. TiO_2-(CaO+MgO)-(SiO_2+Al_2O_3) with Al_2O_3/SiO_2 = 0.60 and MgO/CaO = 0.20

Dicalcium silicate $2(Ca,Mg)O{\cdot}SiO_2$; melilite $2CaO{\cdot}(MgO,Al_2O_3){\cdot}2(SiO_2,Al_2O_3)$; anorthite ($CaO{\cdot}Al_2O_3{\cdot}2SiO_2$), perovskite $CaO{\cdot}TiO_2$, pseudobrookite M_3O_5 and mullite $3(Al,Ti)_2O_3{\cdot}2SiO_2$. The experimental results indicate that merwinite primary phase field disappears when the Al_2O_3/SiO_2 ratio is increased from 0.4 to 0.6 while the MgO/CaO ratio is kept at 0.20.

Section 3. TiO_2-(CaO+MgO)-(SiO_2+Al_2O_3) with Al_2O_3/SiO_2 = 0.40 and MgO/CaO = 0.40

Periclase MgO; merwinite $3CaO{\cdot}MgO{\cdot}2SiO_2$; melilite $2CaO{\cdot}(MgO,Al_2O_3){\cdot}2(SiO_2,Al_2O_3)$; anorthite $CaO{\cdot}Al_2O_3{\cdot}2SiO_2$, perovskite $CaO{\cdot}TiO_2$, pseudobrookite (M_3O_5) and mullite $3(Al,Ti)_2O_3{\cdot}2SiO_2$. It can be seen from Figures 1 and 3 that at the same Al_2O_3/SiO_2 ratio of 0.40 the dicalcium silicate primary phase field is replaced by periclase primary phase field when the MgO/CaO ratio is increased from 0.2 to 0.4.

Section 4. TiO_2-(CaO+MgO)-(SiO_2+Al_2O_3) with Al_2O_3/SiO_2 = 0.40 and MgO/CaO = 0.72

Periclase MgO; spinel $MgO{\cdot}(Al,Ti)_2O_3$; forsterite$2(Mg,Ca)O{\cdot}SiO_2$; anorthite $CaO{\cdot}Al_2O_3{\cdot}2SiO_2$, perovskite $CaO{\cdot}TiO_2$, pseudobrookite (M_3O_5) and mullite $3(Al,Ti)_2O_3{\cdot}2SiO_2$. It can be seen from Figures 3 and 4 that at the same Al_2O_3/SiO_2 ratio of 0.40 the merwinite and melilite primary phase fields are replaced by spinel and forsterite primary phase fields when the MgO/CaO ratio is increased from 0.4 to 0.72.

Relationship between Liquidus Temperature and Basicity (CaO+MgO)/(SiO_2+Al_2O_3) in *TiO_2*-free and *TiO_2*-containing Slags

Liquidus temperatures as a function of basicity (CaO+MgO)/(SiO_2+Al_2O_3) are presented in Figures 5 and 6 for TiO_2 concentrations of 0 and 10 wt%, respectively. In each case 4 isotherms derived from Figures 1 to 4 are presented, respectively. It can be seen from Figure 5 that there are generally 3 zones presented in 4 sections when basicity (CaO+MgO)/(SiO_2+Al_2O_3) is increased from 0 to 1.40. First zone is in mullite primary phase field at low basicity where the liquidus temperatures decrease rapidly with increasing basicity. The second zone is in anorthite primary phase field at medium basicity range in which the liquidus temperatures first increase and then decrease with increasing basicity. At higher basicity the slag is located in silicates (dicalcium silicate, merwinite, melilite and forsterite) or oxides (periclase and spinel) primary phase fields. The liquidus temperatures in this zone gradually increase with increasing the basicity.

Both Al_2O_3/SiO_2 and MgO/CaO ratios in the slag have a significant effect on the liquidus temperature. It can be seen from Figure 5 that the liquidus temperatures for the slag having higher Al_2O_3/SiO_2 weight ratio (0.60) are generally higher than those having lower Al_2O_3/SiO_2

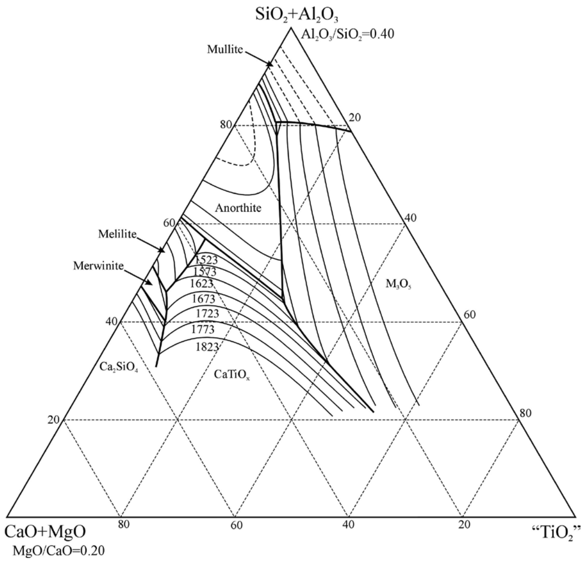

Figure 1: Experimental data obtained on the liquidus of the system CaO-MgO-Al_2O_3-SiO_2-TiO_2 with weight ratios of Al_2O_3/SiO_2=0.40 and MgO/CaO=0.20 at carbon saturation, compositions in wt%, temperatures in K

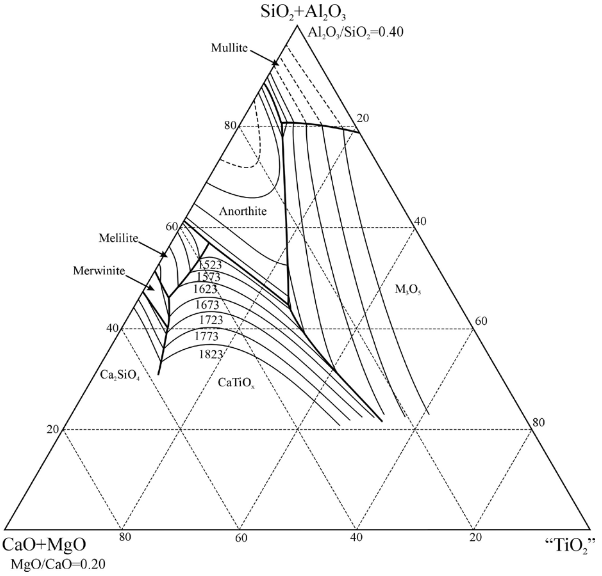

Figure 2: Experimental data obtained on the liquidus of the system $CaO-MgO-Al_2O_3-SiO_2-TiO_2$ with weight ratios of $Al_2O_3/SiO_2=0.60$ and $MgO/CaO=0.20$ at carbon saturation, compositions in wt%, temperatures in K

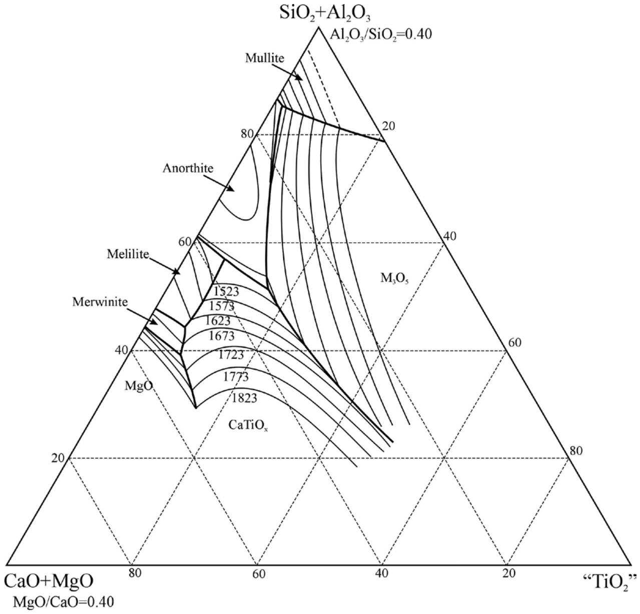

Figure 3: Experimental data obtained on the liquidus of the system $CaO-MgO-Al_2O_3-SiO_2-TiO_2$ with weight ratios of $Al_2O_3/SiO_2=0.40$ and $MgO/CaO=0.40$ at carbon saturation, compositions in wt%, temperatures in K

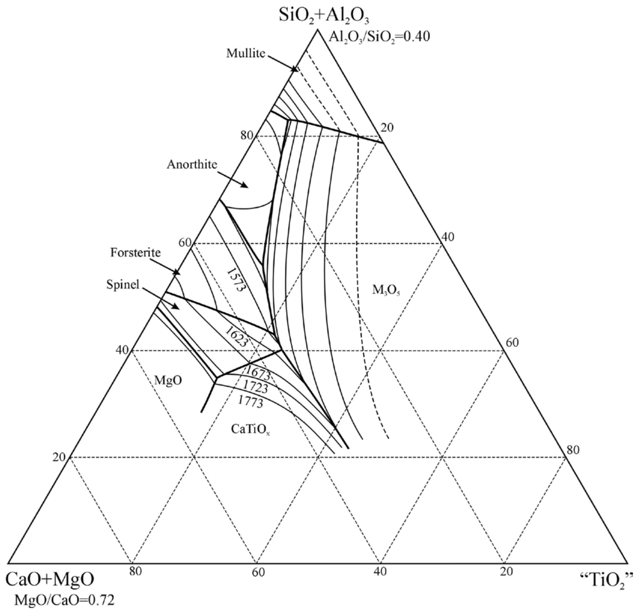

Figure 4: Experimental data obtained on the liquidus of the system CaO-MgO-Al_2O_3-SiO_2-TiO_2 with weight ratios of $Al_2O_3/SiO_2=0.40$ and MgO/CaO=0.72 at carbon saturation, compositions in wt%, temperatures in K

weight ratio (0.40) when the MgO/CaO ratio is the same (0.20). At the same Al_2O_3/SiO_2 ratio of 0.40, the liquidus temperatures do not change significantly with the MgO/CaO ratio in mullite primary phase field (zone 1). In anorthite primary phase field the liquidus temperatures decrease with increasing MgO/CaO ratio. When MgO/CaO ratio is increased from 0.20 to 0.40 the slag is still located in the melilite and merwinite primary phase fields in the basicity range 0.62 to 1.2. The liquidus temperatures decrease slightly with increasing MgO/CaO ratio. However, when the MgO/CaO ratio is increased from 0.40 to 0.72 the anorthite primary phase field is reduced in size and the merwinite and melilite primary phase fields are replaced by spinel and forsterite primary phase fields. The liquidus temperatures in the spinel and forsterite primary phase fields are generally higher than those in merwinite and melilite primary phase fields at the same basicity.

With addition of TiO_2 in the slag the relationship between liquidus temperature and basicity becomes more complex. Addition of 10 wt% TiO_2 in the slag introduced two Ti–containing phases, pseudobrookite (M_3O_5) and perovskite $CaO{\cdot}TiO_2$. The M_3O_5 primary phase field appears in Sections 1, 3 and 4 and is located between mullite and anorthite primary phase fields. The perovskite appears in Sections 1, 2 and 3 and replaced melilite and merwinite phase fields.

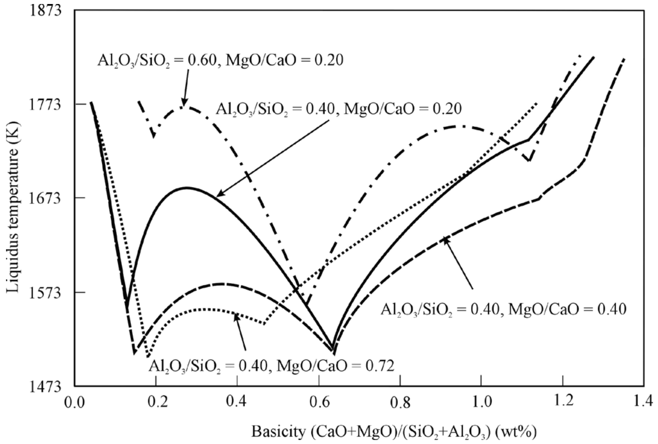

Figure 5: Liquidus temperatures as a function of basicity (CaO+MgO)/(SiO_2+Al_2O_3) at TiO_2–free system

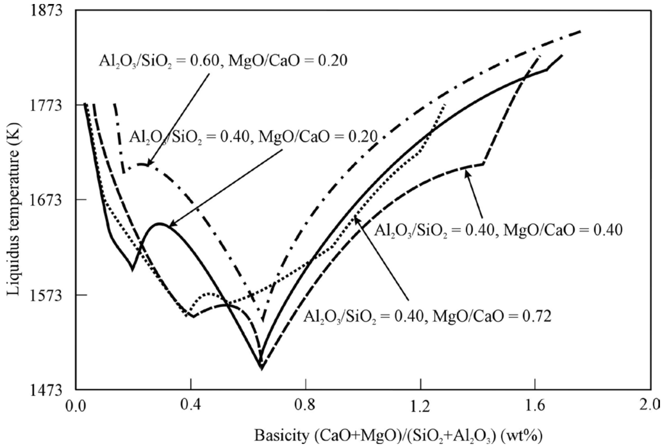

Figure 6: Liquidus temperatures as a function of basicity (CaO+MgO)/(SiO_2+Al_2O_3) at 10 wt% TiO_2

Effect of *TiO_2* on Liquidus Temperature

Another effect of TiO_2 addition is to decrease liquidus temperatures in the whole basicity range investigated. Figure 7 shows the changes of liquidus temperature as a function of TiO_2 concentration at fixed basicities (CaO+MgO)/(SiO_2+Al_2O_3) of 1.0.

It can be seen from Figure 7 that there are generally 3 zones presented in 4 sections in the composition range investigated. In the first zone the primary phase is merwinite for Section 1, melilite for Sections 2 and 3, and spinel for Section 4. In the merwinite and melilite primary phase fields the liquidus temperatures are decreased by 40–100 degrees with additions of 5–8 wt% TiO_2. In the spinel primary phase field the liquidus temperatures decrease relatively slowly with increasing TiO_2 concentration. In the second zone the slag is located in the perovskite primary phase field. The liquidus temperatures in zone 2 first increase and then decrease with increasing TiO_2 concentration. It can be seen that in the second zone the liquidus temperatures can be significantly decreased with increasing MgO/CaO ratio. In the third zone the slag is located in pseudobrookite primary phase field and the liquidus temperatures increase with increasing TiO_2 concentration. It can be seen from Figure 7 that pseudobrookite is formed at much lower TiO_2 (30 wt%) at higher MgO/CaO ratio.

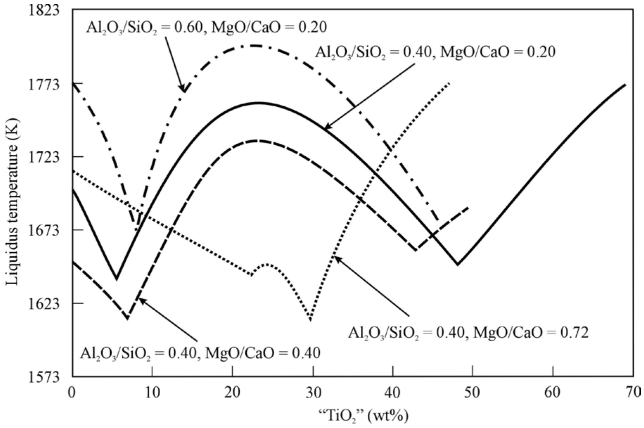

Figure 7: Liquidus temperatures for pseudo-binary section (CaO+MgO+SiO_2+Al_2O_3)– TiO_2 at basicity (CaO+MgO)/(SiO_2+Al_2O_3) = 1.0

Applications of the Phase Diagrams

The present research has provided new information on phase relations and liquidus temperatures in the system CaO-MgO-Al_2O_3-SiO_2-TiO_2 in composition ranges of interest to iron blast furnace practice. These diagrams can be used to explain a number of phenomena that have been observed in previous studies.

A number of workers have investigated the recovery of titania from high-titania iron blast furnace slag through the use of controlled crystallisation and physical separation techniques [33, 34]. Studies by Fu [33] indicated that fine dendritic perovskite crystals were formed for CaO/SiO_2 = 1.0, but large equiaxed crystals were formed for CaO/SiO_2 = 1.4. Dendritic crystals typically are formed during cooling of slags that were fully liquid at equilibration temperature. The larger equiaxed crystals are typically formed by equilibration below the liquidus, in this case in the perovskite primary phase field. From the liquidus surfaces that have been determined in the present study (Figures 1 to 4) it can be seen that the liquidus temperatures in the perovskite primary phase field increase with increasing basicity. As a result, the proportion of the primary crystal is increased at a given temperature.

The overall aim of the current study has been to identify potential slag chemistries that could be used to operate the modified iron blast furnace at lower temperatures than those in existing practice. At this stage in the investigation three significant factors emerge.

Firstly, the liquidus temperatures can be significantly decreased for TiO_2-containing slags with increasing MgO/CaO ratio. In the southwest of China the iron blast furnace titaniferrous slags contain 20–25 wt% TiO_2 [32]. It can be seen from Figure 7 that at basicity (CaO+MgO)/(SiO_2+Al_2O_3) of 1.0 and Al_2O_3/SiO_2 ratio of 0.40 the liquidus temperature is decreased by more than 100 degrees when the MgO/CaO ratio is increased from 0.20 to 0.72.

The second feature is that there is a low temperature region that runs parallel to the (CaO+MgO)-(SiO_2+Al_2O_3) joint at approximately 5–8 wt% TiO_2. This extends from the anorthite primary phase field at the one end, to the Ca_2SiO_4 or MgO primary phase fields at the other. This low temperature region is bounded on one side by the perovskite primary phase field, and melilite and merwinite primary phase fields on the other. The exact position of the local minimum varies slightly with MgO/CaO and Al_2O_3/SiO_2 ratios.

The third feature is that addition of TiO_2 significantly reduces the size of the Ca_2SiO_4 primary phase field. Formation of the Ca_2SiO_4 phase can significantly increase liquidus temperature and results in the transformation of α-Ca_2SiO_4 to α'-Ca_2SiO_4 on cooling producing powder slag. With presence of 10 wt% TiO_2 the Ca_2SiO_4 phase is not formed at basicities below 1.6 for Sections 1 and 2. In fact, the Ca_2SiO_4 primary phase field is replaced by periclase MgO primary phase field when MgO ratio is increased to above 0.4.

These are interesting observations and further systematic investigations of these systems are underway to identify optimum slag compositions that may be used in the low temperature, low energy blast furnaces of the future.

CONCLUSIONS

The liquidus temperatures and phase relations have been experimentally determined in the system CaO-MgO-Al_2O_3-SiO_2-TiO_2 at carbon saturation. The results are presented in a series of pseudo–ternary sections TiO_2-(CaO+MgO)-(SiO_2+Al_2O_3) with fixed MgO/CaO and Al_2O_3/SiO_2 weight ratios.

With addition of TiO_2 to normal iron blast furnace CaO-MgO-SiO_2-Al_2O_3 slag two new phases perovskite $CaO\cdot TiO_2$ and pseudobrookite $[2(Ti^{3+},Mg^{2+}, Al^{3+})\cdot Ti^{4+}O_5)]$ are formed. The liquidus temperatures and primary phase fields in the quinary system are markedly different from the system CaO-MgO-SiO_2-Al_2O_3. The liquidus temperature is shown to be dependent on the (CaO+MgO)/(SiO_2+Al_2O_3), MgO/CaO and Al_2O_3/SiO_2 ratios and TiO_2 concentration. Limited addition of TiO_2 decreases liquidus temperatures of the slag and stability of the Ca_2SiO_4 phase. The liquidus temperatures of the iron blast furnace titaniferrous slags can be significantly decreased with increasing MgO/CaO ratio.

ACKNOWLEDGEMENTS

The authors wish to thank: Australian Research Council through Discovery program for providing the financial support necessary to undertake this project.

Ms Dong Tang, who provided general laboratory assistance and undertook much of the careful sample preparation and equilibration work.

Mr Ron Rasch and Ms Ying Yu of the Centre for Microscopy and Microanalysis at the University of Queensland, who provided support for the electron microprobe X-ray analysis (EPMA) facilities.

REFERENCES

Biswas, A. K. (1981). *Principles of Blast Furnace Ironmaking.* Cootha Publishing, Brisbane. [1]

ISIJ (1987). Blast Furnace Phenomena and Modelling. Elsevier. [2]

Verlag, Eisenh (1995). Slag Atlas, Dusseldorf, 2nd edition, pp. 216. [3]

Muan, A. & Osborne, E. F. (1965). *Phase Equilibria among Oxides in Steelmaking.* Addison-Wesley, pp. 148. [4]

Morizane, Y., Ozturk, B. & Fruehan, R. J. (1999). Metall. Trans. B, Vol. 30B, pp. 29-43. [5]

Yamamoto, R., Nakajima, R., Koyama, Y. & Niiya, K. (1985). Ironmaking Conf. Proc., ISS–AIME, Detroit, MI, Vol. 44, pp. 149-63. [6]

Higuchi, M. (1978). Trans. ISS, I&SM, June, pp. 33-42. [7]

Tomita, Y., Terayama, O., Ohishi, T., Funakoshi, T., Hoshikuma, Y., Nunomura, S. & Hirota, N. (1995). Proc. McMaster Symp. on Iron and Steelmaking, May, No. 23, pp. 32-40. [8]

Koike A., Tanaka, K., Kariya, J., Kojima, M. & Sato, K. (1991). Proc. 2nd Eur. Ironmaking Congr., The Institute of Metals, Glasgow, Sept., pp. 155-167. [9]

Shimomura, K. (1991). Proc. 2nd European Ironmaking Congr., The Institute of Metals, Glasgow, Sept., pp. 179-87. [10]

Datta, K., Sen, P. K., Gupta, S. S. & Chatterjee, A. (1993). Steel Research, Vol. 64, pp. 232-238. [11]

Fine ,H. A. & Arac, S. (1980). Ironmaking and Steelmaking, No. 4, pp. 160-66. [12]

Devries, R. C., Roy, R. & Osborn, E. F. (1955). J. Am. Ceram. Soc., Vol. 38, pp. 158-71. [13]

Ohno, A. & Ross, H. U. (1963). Can. Metall. Q., Vol. 2 (3), pp. 243- 58. [14]

Muan, A., Adv. Ceram. (1988). 3rd meeting, pp. 25-44. [15]

Sakai, H. & Suito, H. (1996). ISIJ International, Vol. 36(2), pp. 138-142. [16]

Lynch, D. C. & Bullard, D. E. (1997). Metall. Trans. B, Vol. 28B, pp. 447-453. [17]

Pelton, A. D., Eriksson, G., Krajewski, D., Goebbels, M. & Woermann, E., Zeitschr. (1998). Phys. Chem., Vol. 207, pp. 163-180. [18]

Petrov, S. A., Shitova, V. I., Mikirticheva, G. A., Grabovenko, L. Y. & Kuchaeva, S. K. (1998). Zhur. Priklad. Khim., Vol.71(4), pp. 547-550. [19]

Ohta, M. & Morita, K. (2002). ISIJ International, Vol. 42(5), pp. 474-481. [20]

Ito, K., Sano, N. (1981). Tetsu to Hagane, Vol. 67, pp. 2131-3137. [21]

Benesch, R., Ledzki, A. & Kopec, R. (1989). Thermochimica Acta, Vol. 152, pp. 447-461. [22]

Morizane, Y., Ozturk, B. & Fruehan, R. J. (1999). Metall. Trans B, Vol. 30B, pp. 385-392. [23]

Jung, S. & Fruehan, R. J. (2001). ISIJ International, Vol. 41(12), pp. 1447-1453. [24]

Ariyo, C. & Holappa, L. (2002). Scand. Met. Quart., Vol. 31, pp. 385-392. [25]

Tramnell, G., Ostrovoski, O. & Jahanshahi, S. (2002). Metall. Trans B, Vol. 33B, pp. 61-67. [26]

Ariyo, C., Gonzales, P. & Holappa, L. (2004). 7th Int'l Conf. Molten Slags, Fluxes and Salts, Capetown, SAIMM, Johannesburg, pp. 125-128. [27]

Handfield, G., Charette, G. G. & Lee, H. Y. (1972). J Metals, Vol. 24 (Sept.), pp. 37-40. [28]

Xie, D., Mao, Y. & Zhu, Y. (2004). 7th Int'l Conf. Molten Slags, Fluxes and Salts, Capetown, SAIMM, Johannesburg, pp. 43-50. [29]

Jak, E. & Hayes, P. C. (2004). 7th Int'l Conf. Molten Slags, Fluxes and Salts, Cape Town, South Africa, SAIMM, Johannesburg, pp. 85-103. [30]

Zhao, B., Jak, E. & Hayes, P. C. (2004). Tenth International Ferroalloys Congress, Cape Town, South Africa, SAIMM, Johannesburg, pp. 184-193. [31]

Li, Z. & Xu, C. (1996). ISIJ International, Vol. 36(3), pp. 279-283. [32]

Fu, N., Zhang, Y. & Sui, Z. (1997). Mining and Metallurgical Engineering, Vol. 17, pp. 36-39. [33]

Wang, X., Mao, Y., Liu, X. & Zhu, Y. (1990). J. of Iron and Steel Research, Vol. 2, pp. 1–6. [34]